Title: Primate neuronal connections are sparse as compared to mouse

Authors: G.A. Wildenberg[1,2*], M.R. Rosen[1], J. Lundell[1], D. Paukner[1], D.J. Freedman[1], N. Kasthuri[1,2]

Affiliations:

[1]Department of Neurobiology, University of Chicago, Chicago, IL, USA.

[2]Argonne National Laboratory, Lemont, IL, USA.

*Correspondence to: gwildenberg@uchicago.edu

Abstract:

Detailing how primate and mouse neurons differ is critical to understanding how brains evolve and for translating findings from mice into humans. However, scarce data about neuronal connections, particularly in primates, makes such comparisons difficult. We use large volume electron microscopy to address this gap, reconstructing 11,415 synapses onto morphologically equivalent adult primate and mouse neurons in Layer 2/3 of primary visual cortex (V1). Neurons from both species distribute in cortex at similar densities, have similar somatic volumes, and dendritic branching patterns, but primate excitatory and inhibitory neurons receive ~4 times fewer excitatory and inhibitory connections than equivalent mouse neurons. The reduction in excitatory inputs is larger, resulting in a 2-fold decreased ratio of excitatory to inhibitory inputs in primate neurons. Finally, despite reductions in inhibitory synapse number, neighboring excitatory primate neurons are co-innervated by inhibitory axons at rates and proportions similar to mouse neurons. We present a first glimpse of large-scale connectivity comparisons across mouse and primate brains which underscore the need for future analyses since such differences likely represent a substantial part of how mouse and primate brains differ.

Main Text:

Ever since Cajal's discovery of the vast menagerie of neuronal cell types in the brain (*1*), neurons have been grouped based on structural, functional, and more recently, molecular and connectivity similarities. Because of its small size, genetic manipulability, and basic mammalian structure, the mouse nervous system serves as an important model for such classifications (*2-4*), and there are industrial scale efforts at classifying all mouse neurons by genetics and their pattern of connections to other neurons. However, 'translating' such findings from mice to primates and ultimately humans will require, at least, a means of associating mouse neuronal cell types and their connectivity patterns to primate neuronal cell types and connectivity patterns. While there is a recent explosion in studies and techniques mapping long and short-range connections in the mouse (*3, 5-8*), there is a large gap in detailing how neurons connect in the primate brain and hence what differences exist relative to the mouse.

Part of the reason for this gap is that many of the genetic tools available in mice are unavailable in primates, and electron microscopy remains the gold standard for delineating neuronal connections. Despite recent advances in large volume, automated serial electron microscopy (EM) (*i.e.* connectomics) (*9-12*), synapse level reconstructions of neural circuits in primate brains would be expensive and pose technical and computational challenges even beyond mouse connectomes (*13-15*). These efforts could be justified if such information provided value beyond what could be more easily inferred from similar ongoing efforts in the mouse. However, since there are few comparisons of how primate and mouse neuron connections differ (*16*), it remains unknown if and how neural circuits in primates differ from circuits in similar regions of the mouse brain. We address this gap using large volume serial EM to compare the numbers and

types of connections received by individual neurons in the primary visual cortex (V1) of mouse (*Mus musculus*) and primate (*Macaca mulatta*).

We prepared 300µm thick sections of primary visual cortex (V1) from adult mouse (15 weeks old) and primate (11 years old) for multi-scale EM-based connectomics. V1 was identified in each species using areal and cellular landmarks (fig. S1, A and B), and samples were prepared as previously described (*17*) (and see **Methods**). We collected 3,000 ultra-thin sections using the ATUM approach (*18*) from mouse (each section: 0.8mm x 1.5 mm x 40nm) and 3,000 from primate (0.8mm x 2.4mm x 40nm), where each individual section spanned all cortical layers in both species (**Fig. 1, A and B**). We imaged the depth of cortex with low resolution EM (~40 nm in plane resolution) and skeletonized the dendritic arbors of 102 primate neurons and 68 mouse neurons across all cortical layers (**Fig. 1, A and B**). We used these reconstructions to evaluate neuronal shapes and densities between species and identify Layer 2/3 (L2/3) in both species for subsequent fine resolution EM (movies S1 and S2, ~ 6nm in plane resolution, 100 μm^2 field of view for 750 sections in mouse, 100 μm^2 field of view for 675 sections in primate).

We first asked about similarities in the shapes and distributions of excitatory neurons. We annotated the location of every neuronal soma in L2/3 in both datasets and traced their dendritic arbors completely in the fine resolution EM volume. We found that excitatory soma were distributed at similar densities across both species (**Fig. 1C**; mean distance between soma: primate, 47.6 µm mean, 0.29 µm SEM, n = 71; mouse, 53.3 µm mean, 0.38 µm SEM, n = 62. P=2.8e-3, Mann-Whitney Test), had similar somatic surface areas (fig. S2A; mean somatic surface area: primate, 386.9 μm^2 mean, 20.8 μm^2 SEM, n = 8; mouse, 369.5 μm^2 mean, 12.4 μm^2 SEM, n = 6. P=0.3, Mann Whitney U test), and number of dendritic branch points (**Fig. 1D**; mean dendritic branch number: primate, 16.2 mean, 1.2 SEM, n = 47 neurons; mouse, 18.0

mean, 0.9 SEM, n = 20 neurons. P=0.0765, Mann-Whitney Test). Finally, we found that the total length of dendrite per neuron was larger in mouse (fig. S2B; mean dendritic length: primate, 398.8 mean, 41.2 SEM, n = 47 neurons; mouse, 682.5 mean, 45.9 SEM, n = 20 neurons. P =1.0e-5, Mann Whitney U test), similar to previous reports (*19*). Visual inspection of the neurons (fig. S3) revealed that the majority of neurons in both species were pyramidal with apical pointing dendrites, and that 3/37 soma in the mouse and 9/42 primate soma were inhibitory neurons, agreeing with previously reported ratios (*20, 21*).

Given their similarity of shape and distributions, we next analyzed whether mouse and primate neurons differed in the number and types of neuronal connections received. We annotated 7,705 synapses and 186 axons that synapsed onto 8 excitatory and 3 inhibitory neurons in the mouse and 3,710 synapses and 84 axons that synapsed on 8 excitatory and 5 inhibitory neurons in the primate (**Fig. 1, E and F**). We classified each synapse as a spine, shaft, somatic, or perisomatic synapse (*22*), and each axon as excitatory or inhibitory based on whether they predominantly innervated spines, or shafts and somas, respectively (see **Methods**, *23*).

We found stark differences in the number of connections received by primate excitatory neurons. In the examples shown in **Figure 2A**, the primate neuron had, on average, 0.37 spine synapses/µm of dendrite while that density was three-fold higher in the mouse, 1.15 spine synapses/µm (**Fig 2A,** lower panel and right inset). Similarly, the example mouse soma received 66 somatic and perisomatic synapses while the primate received 20; a three-fold increase in the mouse (**Fig. 2A,** lower panel and right inset). Across neurons, spine synapse density increased with the distance from the soma in both species and reached significantly greater density in the mouse than in the primate (**Fig. 2B**; mean spine synapse density: primate, 0.55 synapses/µm mean, 0.04 synapses/µm SEM, n = 109 10µm dendrite fragments across 10 neurons; mouse, 1.34

synapses/µm mean, 0.09 synapses/µm SEM, n = 82 dendrite fragments across 10 neurons. P=1.5E-11, Mann-Whitney U test). The average number of somatic and perisomatic synapses for mouse neurons was 3.8-fold higher compared to primate excitatory neurons (**Fig. 2C**; synapses/soma: mouse, 102.2 mean, 5.3 SEM, n = 388 synapse across 6 soma; primate, 26.9 mean, 2.0 SEM, n = 129 synapses across 8 soma. P=6.6E-4, Mann-Whitney).

We next looked at shaft synapses (*i.e.* synapses on dendritic shafts between spines) and the number of spines receiving multiple synapses. The density of shaft synapses was reduced relative to spine synapses in both species, and unlike primary spine and somatic synapses, primate and mouse neurons had similar densities of shaft synapses (fig**.** S4; shaft synapses density: primate, 0.19 synapses/µm mean, 0.02 synapses/µm SEM, n = 109 10 µm dendrite fragments counted across 10 neurons; mouse, 0.18 synapses/µm mean, 0.02 synapses/µm SEM, n = 82 10 µm dendrite fragments counted across 10 neurons. P=0.17, Mann-Whitney U test). However, despite having fewer spines, primate excitatory neurons receive three-fold more second spine synapses (**Fig. 2D;** number of 2nd spine synapses: primate, 0.11 2nd synapses/spine mean, 0.001 2nd synapses/spine SEM, n = 180 spines across 3 neurons; mouse, 0.03 2nd synapses/spine mean, 0.00 2nd synapse/spine SEM, n = 180 spines across 3 neurons. P = 7.1e-3, Mann-Whitney U test). The majority of these 'second' spine synapses have been reported to likely be inhibitory based on immunoreactivity for GABA (*24-26*) and we find similar results: the majority of second spine synapses in primates lack a clear post-synaptic density and have smaller vesicles, consistent with inhibitory synapses (**Fig. 2D**). Finally, using these spine, shaft, somatic, and second spine averages and mean dendritic arbor lengths for primate and mouse layer 2/3 neurons as previously reported (*19*), we calculated the ratio of the total number of excitatory and inhibitory inputs onto individual excitatory neurons (see **Methods**). We found that mouse neurons received on average

6894.5 ± 647 (SEM) total connections with 5846.5 ± 626 (SEM) excitatory and 1048.0 ± 22 (SEM) inhibitory connections. Primate excitatory neurons received on average 2499.6 ± 557 (SEM) total connections with 1697.6 ± 507 (SEM) excitatory and 802.0 ± 50 (SEM) inhibitory connections. Thus, primate neurons had lower E/I ratios than mouse neurons (**Fig. 2E**; E/I ratio: mouse, 5.55 mean, 0.48 SEM, n = 770 1st spine synapses of which 180 were scored for 2nd synapses, 109 shaft synapses, and 401 somatic/perisomatic synapses over 4 neurons; primate, 2.03 mean, 0.48 SEM, n = 427 spine synapses of which 180 were scored for 2nd spine synapses, 151 shaft synapses,106 somatic/perisomatic synapses over 4 neurons. P=0.029, Mann-Whitney U test).

We next asked similar questions about inhibitory neurons in the same volume (fig. S3). In the examples shown in **Figure 3A**, the mouse inhibitory neuron had a 1.45-fold higher dendritic shaft synapse density (3.00 synapses/µm) compared to the primate neuron (2.06 synapses/µm). There was also a 4-fold difference in the number of somatic synapses, with the mouse inhibitory neuron receiving 162 somatic synapses compared to 39 in the primate (**Fig. 3A,** bottom panel and right inset). Across multiple neurons, mouse inhibitory neurons had ~1.5x fold more shaft synapses than primate inhibitory neurons (**Fig. 3B**; shaft synapse density: primate, 1.87 synapses/µm mean, 0.17 synapses/µm SEM, n = 29 10µm dendritic fragments across 5 neurons; mouse, 2.70 synapses/µm mean, 0.12 synapses/µm SEM, n = 39 10 µm dendrite fragments across 4 neurons. P=0.0012, Mann-Whitney U test). Likewise, mouse inhibitory neurons have on average more somatic and perisomatic synapses than primate neurons (**Fig. 3C**; number of somatic/perisomatic synapses: mouse, 247.7 synapses/soma mean, 14.8 synapses/soma SEM, n = 743 synapses across 3 soma; primate, 44.5 synapses/soma mean, 6.7 synapses/soma SEM, n = 178 synapses across 4 soma. P=0.029, Mann-Whitney U test). Finally, we asked about relative

contribution of excitatory and inhibitory inputs on the dendrites (*27, 28*) of matched inhibitory neurons (*i.e.* basal oriented axon). We traced 32 axons in the mouse and 24 axons in the primate that innervated the dendrites of matched inhibitory neurons and annotated every synapse those axons made in the volume. We then classified axons as excitatory if they made predominantly spine synapses or inhibitory if they made predominantly shaft and soma synapses (see Methods). The E/I ratio on the dendrite of mouse inhibitory neurons is 29/3 (~9.7), and 19/5 (~3.8) in primate, a two-fold reduction similar to the differences in the E/I ratios we observed in excitatory neurons (see **Fig. 2E**).

We next asked about species differences in how neurons were wired together, focusing on putative inhibitory axons innervating the soma of primate and mouse excitatory neurons (*29-31*). First, we found that the basic properties of mouse and primate inhibitory axons, like branching, bouton size, and total synapse frequency (*e.g.* somatic, shaft, and spine) were similar between species (fig. S5, A-C). Second, the reduction in the number of synapses on primate neurons was associated with fewer axons innervating primate excitatory neurons than mouse (fig. S5D; axons per soma: primate, 14.0 axons/soma mean, 1.0 axons/soma SEM, n = 84 axons innervating 6 soma; mouse, 37.8 axons/soma mean, 2.5 axons/soma SEM, n = 198 axons innervating 5 soma. P=2.1e-3, Mann-Whitney U test), and that individual axons in both species make on average similar numbers of somatic synapses on primate and mouse neurons (fig. S5E; number of somatic synapses per axon: primate, 1.33 soma synapses/axon mean, 0.15 soma synapses/axon SEM, n = 115 synapses across 60 axons; mouse, 2.34 soma synapses/axon mean, 0.11 soma synapses/axon SEM, n = 381 synapses across 163 axons. P=0.071, Mann-Whitney U test).

We next tested the hypothesis that the large reduction in the number of axons innervating primate neurons with little difference in the basic properties of axons would result in marked

differences in how these axons innervated multiple target neurons. We first asked how often do nearest neighbor excitatory neurons in the two species 'share' somatic input from the same axon? We traced every axon innervating the somas of nearest neighbor excitatory neurons in both species and analyzed the number of inhibitory axons 'shared' with the neighboring soma. In **Figure 4A**, we show 19 axons making 40 synapses on two nearest neighbor primate neuronal somas and 57 axons making 151 synapses on two nearest neighbor mouse neuronal somas. Despite the large difference in absolute numbers, the fraction of somatic axons that innervated both soma – 'shared' - were equivalent, if not slightly larger, in the primate: 7/19 axons shared, 37% in primate and 14/57 axons shared, 25% in mouse. We observed this trend broadly: inhibitory axons are 'shared' by neighboring excitatory neurons in primate brains at similar, if not slightly higher, rates than in mouse (**Fig. 4B**; frequency of shared axons: primate, 0.40 shared axons mean, 0.02 shared axons SEM, n = 60 axons making 162 synapses across 3 neighboring neuron pairs; mouse, 0.21 shared axons mean, 0.02 shared axons SEM, n = 188 axons making 504 synapses across 3 pairs. P=0.1, Mann-Whitney U test). We then extended this analysis beyond nearest-neighbor neurons to ask: how often do axons innervating a particular soma also synapse with the other excitatory neurons in the volume as a function of somatic distance (*cartoon*, **Fig. 4C**). We identified every synapse (spine, shaft, somatic, or perisomatic) these axons made, starting from a central neuron (n= 4 neurons, 2 primate - P1 and P2- and 2 mouse- M1 and M2), with every other excitatory neuron in the volume. We plotted the number of axons shared between central neurons and other neurons versus distance and found a similar decrease in axonal sharing with distance (**Fig. 4C;** primate P1: n = 10 axons making 145 synapses across 36 neurons, primate P2: n = 9 axons making 103 synapses across 36 neurons; mouse M1: n = 32 axons making 455 synapses across 49 neurons, mouse M2: n = 25 axons making 397 synapses

across 49 neurons). Neurons from both species showed a sharp decrease in sharing: by 70 μm distance from the central soma, few if any axons were shared in either species. Thus, we were unable to disprove our hypothesis that changes in the absolute numbers of connections would correlate with differences in wiring across species.

In this report, we leveraged recent advances in automated serial EM to complete the largest volume 'connectome' in primate primary visual cortex to compare with a connectome of morphologically and functionally similar neurons in the mouse primary visual cortex. Our results show a striking trend of reduced connectivity in individual primate L2/3 neurons relative to their mouse counterparts. This sparsity of connectivity is broad (Table S1): it is evident in both excitatory and inhibitory inputs on excitatory and inhibitory neurons, and reduces the E/I ratio of primate excitatory and inhibitory neurons relative to the mouse. Interestingly, we find that, despite these reductions, aspects of how neurons connect to others, like the degree to which inhibitory inputs innervate nearby neurons are similar across species. Since few or any of these results could have been reliably inferred from either current EM reconstructions of mouse cortex or from comparisons of functional response properties of neurons across species, we conclude that accurately translating mouse connectomes to humans will at least initially require similar volumes of primate brains. Our efforts at mapping connectivity closely parallel and complement genetic/transcriptomic and functional comparisons of individual neurons across mouse, non-human primate and human brains (*32, 33*).

References:

1. S. Ramon y Cajal, P. Pasik, T. Pasik, *Texture of the nervous system of man and the vertebrates*. (Springer, Wien ; New York, 1999).

2. Y. N. Billeh *et al.*, Systematic Integration of Structural and Functional Data into Multi-scale Models of Mouse Primary Visual Cortex. *Neuron* 106, 388-403.e318 (2020).

3. S. W. Oh *et al.*, A mesoscale connectome of the mouse brain. *Nature* 508, 207-214 (2014).

4. U. Knoblich, L. Huang, H. Zeng, L. Li, Neuronal cell-subtype specificity of neural synchronization in mouse primary visual cortex. *Nat Commun* 10, 2533 (2019).

5. A. Motta *et al.*, Dense connectomic reconstruction in layer 4 of the somatosensory cortex. *Science* 366, (2019).

6. J. L. Morgan, J. W. Lichtman, An Individual Interneuron Participates in Many Kinds of Inhibition and Innervates Much of the Mouse Visual Thalamus. *Neuron* 106, 468-481.e462 (2020).

7. A. Karimi, J. Odenthal, F. Drawitsch, K. M. Boergens, M. Helmstaedter, Cell-type specific innervation of cortical pyramidal cells at their apical dendrites. *Elife* 9, (2020).

8. J. A. Bae *et al.*, Digital Museum of Retinal Ganglion Cells with Dense Anatomy and Physiology. *Cell* 173, 1293-1306.e1219 (2018).

9. V. Baena, R. L. Schalek, J. W. Lichtman, M. Terasaki, Serial-section electron microscopy using automated tape-collecting ultramicrotome (ATUM). *Methods Cell Biol* 152, 41-67 (2019).

10. W. Yin *et al.*, A Petascale Automated Imaging Pipeline for Mapping Neuronal Circuits with High- throughput Transmission Electron Microscopy. (2019).

11. K. J. Hayworth *et al.*, Gas cluster ion beam SEM for imaging of large tissue samples with 10 nm isotropic resolution. *Nat Methods* 17, 68-71 (2020).

12. M. Januszewski *et al.*, High-precision automated reconstruction of neurons with flood-filling networks. *Nat Methods* 15, 605-610 (2018).

13. S. M. Plaza, L. K. Scheffer, D. B. Chklovskii, Toward large-scale connectome reconstructions. *Curr Opin Neurobiol* 25, 201-210 (2014).

14. J. W. Lichtman, H. Pfister, N. Shavit, The big data challenges of connectomics. *Nat Neurosci* 17, 1448-1454 (2014).

15. M. A. H *et al.*, Conneconomics: The Economics of Dense, Large-Scale, High-Resolution Neural Connectomics. (2014).

16. A. Hsu, J. I. Luebke, M. Medalla, Comparative ultrastructural features of excitatory synapses in the visual and frontal cortices of the adult mouse and monkey. *J Comp Neurol* 525, 2175-2191 (2017).

17. Y. Hua, P. Laserstein, M. Helmstaedter, Large-volume en-bloc staining for electron microscopy-based connectomics. *Nat Commun* 6, 7923 (2015).

18. N. Kasthuri *et al.*, Saturated Reconstruction of a Volume of Neocortex. *Cell* 162, 648-661 (2015).

19. J. P. Gilman, M. Medalla, J. I. Luebke, Area-Specific Features of Pyramidal Neurons-a Comparative Study in Mouse and Rhesus Monkey. *Cereb Cortex* 27, 2078-2094 (2017).

20. K. T. Sultan, S. H. Shi, Generation of diverse cortical inhibitory interneurons. *Wiley Interdiscip Rev Dev Biol* 7, (2018).

21. D. Džaja, A. Hladnik, I. Bičanić, M. Baković, Z. Petanjek, Neocortical calretinin neurons in primates: increase in proportion and microcircuitry structure. *Front Neuroanat* 8, 103 (2014).

22. T. F. Freund, I. Katona, Perisomatic inhibition. *Neuron* 56, 33-42 (2007).

23. K. M. Harris, R. J. Weinberg, Ultrastructure of synapses in the mammalian brain. *Cold Spring Harb Perspect Biol* 4, (2012).

24. G. W. Knott, C. Quairiaux, C. Genoud, E. Welker, Formation of dendritic spines with GABAergic synapses induced by whisker stimulation in adult mice. *Neuron* 34, 265-273 (2002).

25. E. G. Jones, T. P. Powell, Morphological variations in the dendritic spines of the neocortex. *J Cell Sci* 5, 509-529 (1969).

26. T. Kwon *et al.*, Ultrastructural, Molecular and Functional Mapping of GABAergic Synapses on Dendritic Spines and Shafts of Neocortical Pyramidal Neurons. *Cereb Cortex* 29, 2771-2781 (2019).

27. H. Hioki *et al.*, Cell type-specific inhibitory inputs to dendritic and somatic compartments of parvalbumin-expressing neocortical interneuron. *J Neurosci* 33, 544-555 (2013).

28. O. K. Swanson, A. Maffei, From Hiring to Firing: Activation of Inhibitory Neurons and Their Recruitment in Behavior. *Front Mol Neurosci* 12, 168 (2019).

29. Z. F. Kisvárday, K. A. Martin, D. Whitteridge, P. Somogyi, Synaptic connections of intracellularly filled clutch cells: a type of small basket cell in the visual cortex of the cat. *J Comp Neurol* 241, 111-137 (1985).

30. P. Somogyi, D. K.-T. L. a. C. D. Gilbert, Ed. ((Texas, USA: Portfolio Pub Co), Neural Mechanisms of Visual Perception: Proceedings of the Second Retina Research Foundation Symposium , ed, 1989), pp. 35-62.

31. F. Karube, Y. Kubota, Y. Kawaguchi, Axon branching and synaptic bouton phenotypes in GABAergic nonpyramidal cell subtypes. *J Neurosci* 24, 2853-2865 (2004).

32. A. Bernard *et al.*, Transcriptional architecture of the primate neocortex. *Neuron* 73, 1083-1099 (2012).

33. R. D. Hodge *et al.*, Conserved cell types with divergent features in human versus mouse cortex. *Nature* 573, 61-68 (2019).

34. G. Paxinos, *The rhesus monkey brain in stereotaxic coordinates*. (Academic, Amsterdam ; Boston ; London, ed. 2nd, 2009), pp. 410 p., [302] p. of plates.

35. A. Marx, C. Backes, E. Meese, H. P. Lenhof, A. Keller, EDISON-WMW: Exact Dynamic Programing Solution of the Wilcoxon-Mann-Whitney Test. *Genomics Proteomics Bioinformatics* 14, 55-61 (2016).

Fig. 1.

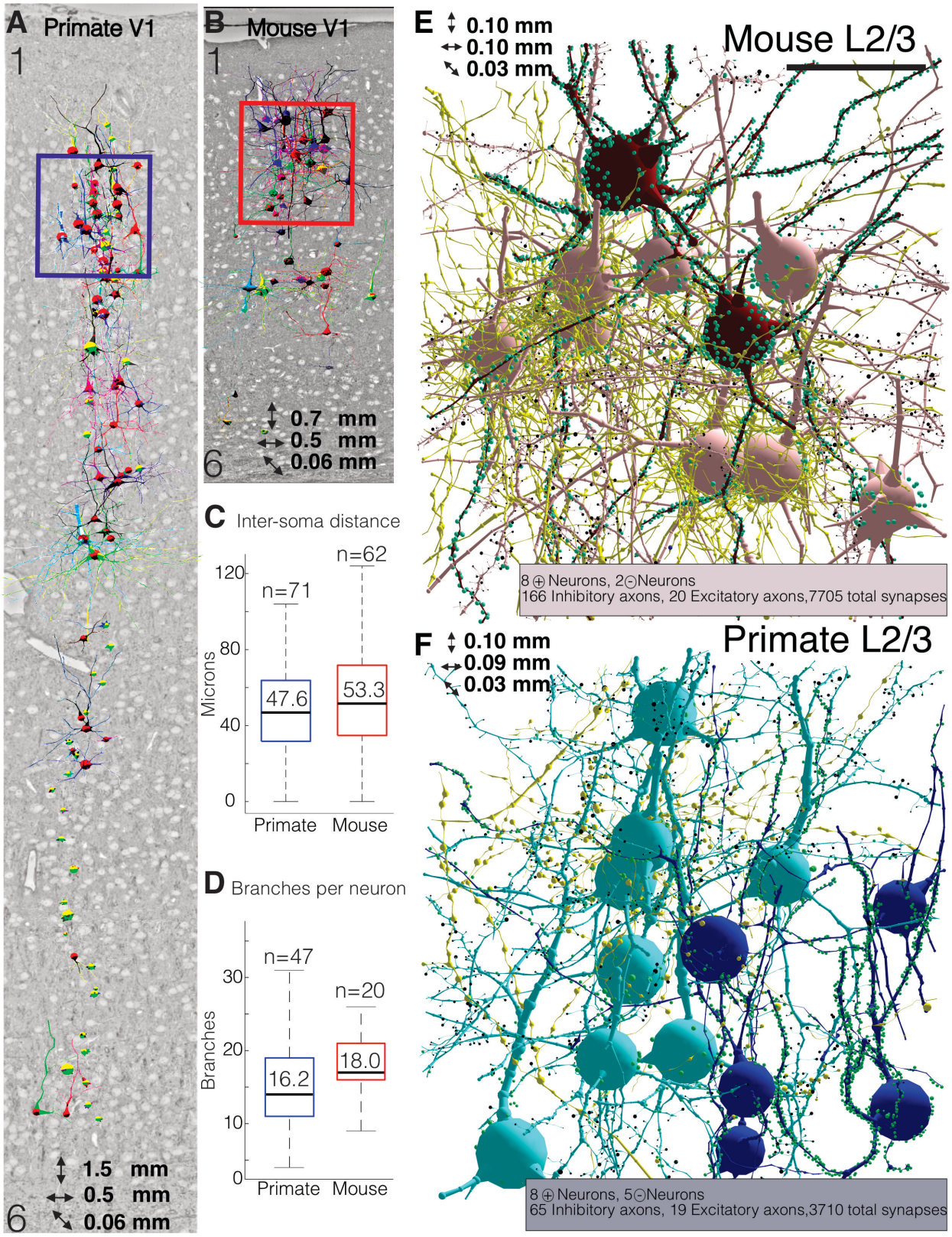

Fig. 1. Similar meso-scale architectures of primary visual cortex (V1) in macaque and mouse. (A-B) Reconstructions of 83 primate (A) and 68 mouse (B) neurons from primary visual cortex (V1), superimposed in place on single EM sections spanning layers 1-6. Blue and red boxes indicate regions of fine resolution imaging. (**C**) Box-and-whisker plot of distances between L2/3 neuronal soma in primate and mouse (primate: 47.6 ± 0.29 µm, n = 71; mouse: 53.3 ± 0.38 µm, n = 62, P=2.8e-3). (**D**). Box-and-whisker plot of dendritic branch number of L2/3 neurons (primate: 16.2 ± 1.2, n= 47; mouse: 18.0 ± 0.9, n= 20, P=0.0765). (**E-F**). 3D reconstructions of mouse (0.10 x 0.10 x 0.03 mm) and primate (0.10 x 0.09 x 0.03 mm) V1, L2/3 sub-volumes re-imaged at fine (~ 6nm XY) resolution. Excitatory neurons (+Neurons) are light red or blue and inhibitory neurons (-Neurons) are dark red or blue in mouse and primate, respectively. Green nodes are inhibitory synapses on shafts and soma, black nodes are excitatory synapses on dendritic spines, fine yellow skeletons are axons. Total reconstructions shown are listed. Scale bar = 50 µm. Data: mean ± SEM. *P*-values: two-tailed Mann-Whitney U test.

Fig. 2.

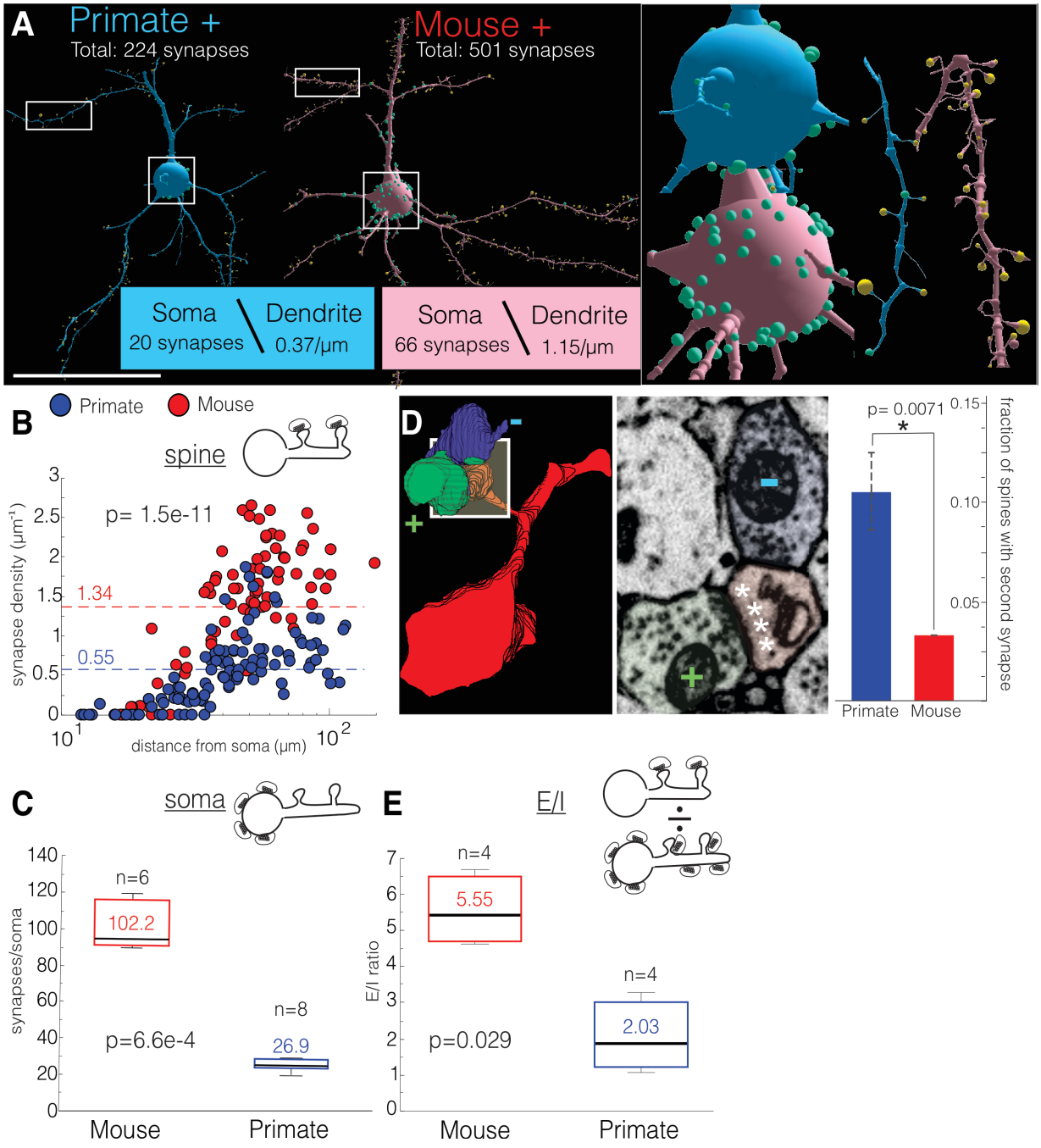

5

Fig. 2 Mouse L2/3 excitatory neurons receive more connections than primate neurons. (**A**) Representative EM reconstructions of morphologically matched L2/3 primate and mouse excitatory (+) neurons. All synapses were annotated and quantified (soma: total # of synapses, dendrite: spine synapses/µm). *Inset*: magnified views of soma and dendrites: shaft and soma synapses are green spheres and spine synapses are yellow spheres. (**B**) Scatter plot of spine synapses/µm versus distance from soma (µm) (primate: 0.55 ± 0.04 synapses/µm, n = 109 10µm dendrite fragments across 10 neurons; mouse: 1.34 ± 0.09 synapses/µm, n = 82 10µm dendrite fragments across 10 neurons; P=1.5e-11). (**C**) Box-and-whisker plot of synapses/soma (mouse: 102.2 ± 5.3, n = 388 synapse across 6 soma; primate: 26.9 ± 2.0, n = 129 synapses across 8 soma; P=6.6e-4). (**D**) Primate excitatory neurons have more 2nd synapses. *Left and middle panel*: 3D reconstruction and 2D EM image of a primate dendritic spine (red) with a 2nd synapse: an excitatory synapse on the spine head (green/+) and inhibitory synapse on the side (blue/-). Asterisks in middle panel show the post-synaptic density on the (+) synapse. *Right panel*: bar plot of the fraction of spines with 2nd synapses (primate: 0.11 ± 0.001, n = 180 spines across 3 neurons; mouse: 0.03 ± 0.00, n = 180 spines across 3 neurons; P = 7.1e-3). (**E**) Box-and-whisker plot of the excitatory to inhibitory synapse (E/I) ratio on excitatory neurons (see Methods) (mouse: 5.55 ± 0.48, n= 770 spine synapses (180 scored for 2nd spine synapses), 109 shaft synapses, and 401 somatic/perisomatic synapses over 4 neurons; primate: 2.03 ± 0.48, n = 427 spine synapses (180 scored for 2nd spine synapses), 151 shaft synapses,106 somatic/perisomatic synapses over 4 neurons; P = 0.029). Scale bar = 45 µm. Data: mean ± SEM. *P*-values: two-tailed Mann-Whitney U test.

Fig. 3.

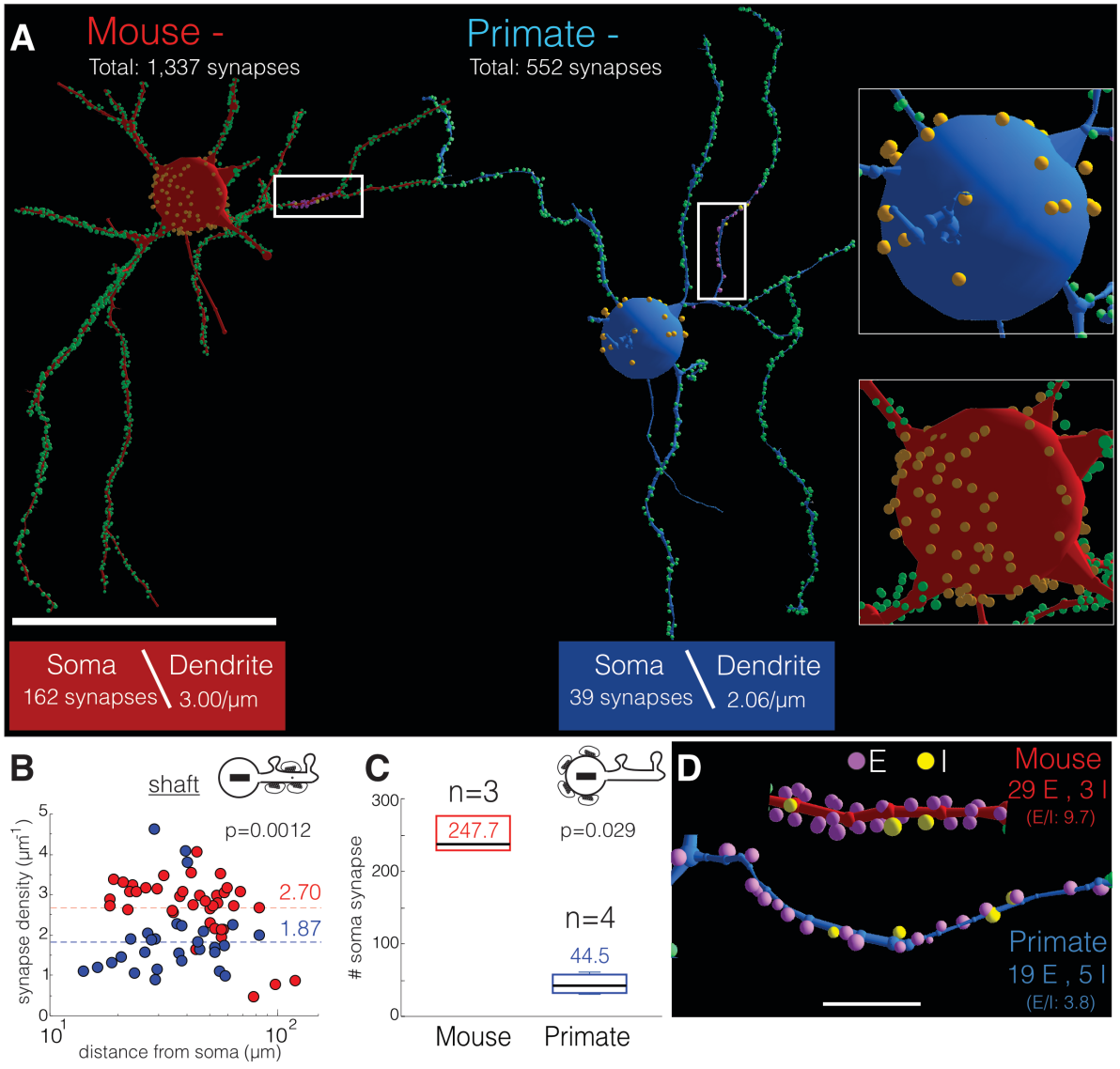

Fig 3. Mouse L2/3 inhibitory neurons receive more connections than primate neurons. (**A**) Representative EM reconstructions of morphologically matched L2/3 mouse and primate inhibitory (-) neurons. All synapses were annotated and quantified (soma: total # of synapses, dendrite: shaft synapses/µm). *Inset*: magnified views of soma and dendrites: soma and shaft synapses as orange and green spheres, respectively. White boxes show regions of detailed analysis performed in (D). (**B**) Scatter plot of shaft synapses/µm versus distance from soma (µm) (primate: 1.87 ± 0.17 synapses/µm, n = 29 10µm dendritic fragments across 5 neurons; mouse: 2.70 ± 0.12 synapse/µm, n = 39 10µm dendrite fragments across 4 neurons; P=0.0012). (**C**) Box-and-whisker plot of synapses/soma (mouse: 247.7 ± 14.8, n = 743 synapses across 3 soma; primate: 44.5 ± 6.7, n = 178 synapses across 4 soma; P=0.029). (**D**) Reconstructions of excitatory (purple spheres) and inhibitory (yellow spheres) synapses along the dendrite of mouse (red) and primate (blue) inhibitory neurons. Mouse neurons have 29 excitatory synapses for every 3 inhibitory (E/I = 9.7), and primate have 19 excitatory synapses for every 5 inhibitory (E/I = 3.8). Scale bars (A**)** 45 µm, (B) 5 µm. Data: mean ± SEM. *P*-values: two-tailed Mann-Whitney U test.

Fig. 4.

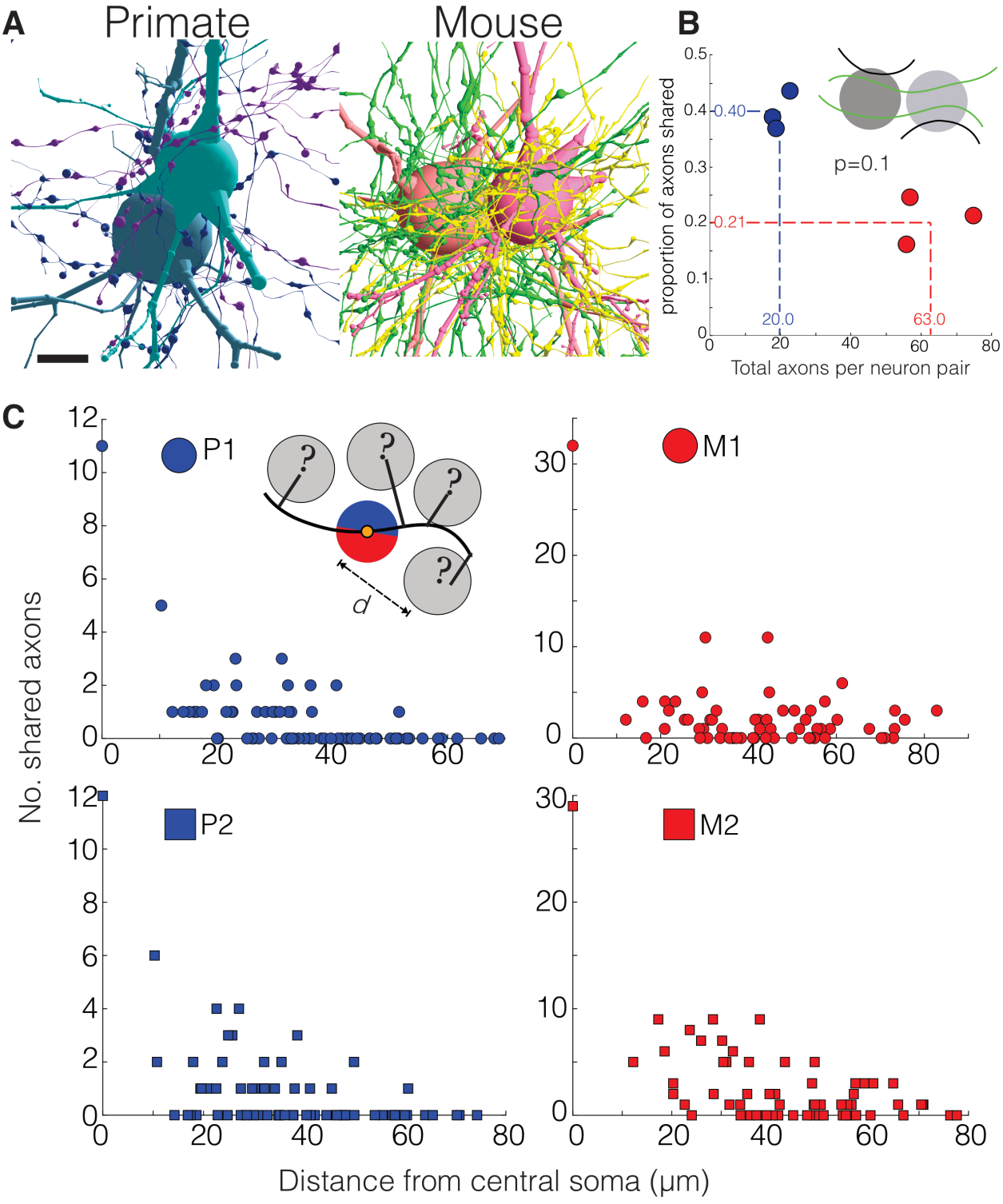

Fig. 4. Neighboring primate and mouse excitatory neurons have similar inhibitory networks. (**A**) Reconstructions of every inhibitory axon innervating the soma of two adjacent L2/3 excitatory neurons (primate: 19 axons, 40 synapses; mouse: 57 axons, 151 synapses). (**B**) *Inset:* shared (green lines) and unshared axons (black lines) between neighboring neuron pairs. Scatter plot of the number of axons synapsed with the soma and perisoma of neighboring neuron pairs versus the proportion of those axons shared between the two neurons (primate: 0.40 ± 0.02 shared axons, n = 60 axons making 162 synapses across 3 neuron pairs; mouse: 0.21 ± 0.02 shared axons, n = 188 axons making 504 synapses across 3 neuron pairs; P=0.1). (**C**) *Inset*: the number of shared axons between a central neuron (blue/red circle) and all neighboring neurons plotted against their distance from the central soma (*d*). Scatter plot showing two analyses for each species (primate: P1, n = 10 axons, 145 synapses, 36 neurons, P2, n = 9 axons, 103 synapses, 36 neurons; mouse: M1, n = 32 axons, 455 synapses, 49 neurons, M2, n = 25 axons, 397 synapses, 49 neurons). Scale bar = 15 µm. Data: mean ± SEM. *P*-values: two-tailed Mann-Whitney U test.